Journal of Marine Research, 71, 399–423, 2013

Seasonal, 2-D sedimentary extracellular enzyme activities and controlling processes in Great Peconic Bay, Long Island

by Zhenrui Cao[1], Qingzhi Zhu[1], Robert C. Aller[1,2], Josephine Y. Aller[1], and Stuart Waugh[1]

ABSTRACT

Extracellular enzymes (EE) initiate heterotrophic remineralization by hydrolyzing high-molecular-weight organic matter to substrates that are sufficiently small (approximately 600 Da) to be transported across cell membranes. An accurate understanding of EE associated remineralization processes in sedimentary deposits requires measuring patterns of extracellular enzyme activity (EEA) with minimal disturbance of natural sediment structure. In this study, two-dimensional patterns of extracellular enzyme (leucine aminopeptidase) activity in shallow-water, marine sediments from Great Peconic Bay, Long Island, New York were examined seasonally at sub-millimeter resolution by using a newly developed EE planar fluorosensor. Comparisons of spatially averaged, vertical enzyme activity profiles measured using this imaging sensor system and traditional sediment homogenization techniques verified the overall consistency of the methodology. The depth-averaged EEA (approximately 10 cm) varied seasonally with highest levels in the late spring through summer (0.2 μmol substrate g-wet-wt^{-1} hr^{-1}) and lowest in the late fall and early winter (0.1 μmol substrate g-wet-wt^{-1} hr^{-1}). EEA distributions, however, showed extensive small-scale horizontal heterogeneity as well as vertical variations. Both the input of reactive substrates (planktonic organic matter) and temperature differences accounted for major changes in EEA seasonally. In general, horizontal heterogeneity in EEA was greatest during warm seasons (summer, fall) as a result of increased macrofaunal activity. On the other hand, vertical variations are less significant during warm periods compared with cold periods as the sediment is more intensely reworked. Hot spots of elevated microbial activity from sub-millimeter to millimeter scales are observed in some seasons and are specifically associated with substrate inputs from phytoplankton blooms and particle reworking by infauna. The deposition of phytodetritus from an early spring bloom greatly enhanced surface sediment EEA, and at this time high EEA closely coincided with regions of elevated metabolite production as measured by NH_4^+ and ΣCO_2 concentrations. Direct correlations between averaged EEA distributions and nutrient production rates were observed throughout the year but no correlations between EEA and pore water nutrient concentrations were present. Spatially resolved EEA directly tracks reactive particle distributions and is generally independent of solute transport mechanisms, such as bioirrigation, and redox conditions.

1. School of Marine and Atmospheric Sciences, Stony Brook University, Stony Brook, New York, 11794-5000 U.S.A.

2. Corresponding author ***e-mail: robert.aller@stonybrook.edu***

1. Introduction

In most marine ecosystems, a large portion of energy and nutrient flow is channeled through the microbial community. The recycling of organic matter starts with the consumption and degradation of detrital organic carbon by a diverse community of heterotrophic microorganisms. Due to their small sizes, however, microbes cannot assimilate molecules larger than approximately 600 Da (Weiss et al., 1991). High molecular weight organic materials must be fragmented by extracellular enzymes (EE) before being incorporated into cells. EE catalyzed hydroxylation is thus a crucial initial step in organic matter remineralization, and in many environments it might be the rate limiting step (Arnosti et al., 1994; Burdige and Gardner, 1998). Understanding rates of extracellular enzymatic activity (EEA) as well as the factors that control enzyme production, performance and distribution are essential to carbon cycling budgets in marine ecosystems (Arnosti, 2011; Boetius and Lochte, 1994). Thus a number of studies of EEA and controlling mechanisms have been conducted over the past decades in a wide range of marine environments from tropical to polar regions (Arnosti, 2011; Chrost, 1991; Hoppe et al., 2002), and in both water columns (Baltar et al., 2009; Hoppe, 2003; Huston and Deming, 2002) and sediments (Boetius and Lochte, 1994; Mayer, 1989; Meyerreil, 1986). Compared to the water column, there are far fewer investigations of EEA in sediments (Arnosti, 2011), despite the fact that EEA in sediments is typically two to three orders of magnitude higher than in overlying water (Hoppe et al., 2002). This disparity is mainly due to the physical and chemical complexity of the sediment matrix, making EEA measurements more complicated and thus more problematic. Traditional methods typically involve dilution of sediment with seawater into slurries which destroys the physical structure of the sediment and leads to potential overestimation of EEA. New techniques with fewer artifacts are required for accurate sediment EEA studies (Arnosti, 1995).

In addition, surface sediments, especially those underlying oxygenated waters, normally display substantial small-scale (mm to cm) spatial and temporal heterogeneity. Organic rich surface sediment typically possesses sharp vertical gradients of O_2, pCO_2, labile organic substrates, and other biogeochemical properties as a consequence of early diagenetic reactions. Furthermore, the activities of benthic flora and macrofauna create a complex, three-dimensional mosaic of redox zones and labile substrates that make sediment heterogeneity much greater than in overlying seawater (Aller, 1994; Hulthe et al., 1998; Papaspyrou et al., 2006). Understanding the influence of such small-scale heterogeneity on organic matter distributions and decomposition is fundamental for more accurate estimation of carbon flux through surface sediments. Traditional EEA measurement techniques, however, are incapable of characterizing the distributions of reactions at high spatial or temporal resolution.

Over the past ten years, planar optical sensors have been applied to quantify chemical distributions in marine sediment with high spatial and temporal resolution, and have documented significant small-scale heterogeneities (Glud, 2008; Glud et al., 1996; Glud et al., 2009; Glud et al., 2001; Wenzhofer and Glud, 2004; Zhu et al., 2005; Zhu et al., 2006). For example, Zhu et al. (2006) used a two-dimensional planar fluorosensor to study sediment pCO_2 distributions in bioturbated sediment, revealing heterogeneity at the sub-millimeter

scale. Glud (2008) applied continuous O_2 imaging showing that short-lived anoxic microniches developed during the degradation of 1- to 2-mm diatom aggregates within an otherwise oxic sediment. Such small-scale patterns and events are normally impossible to capture by traditional measurements, but were revealed by planar sensors. A novel thin-layer foil for a planar optical sensor was also recently developed to resolve heterogeneous patterns of EEA in sediments (Cao et al., 2011). This new system is capable of imaging two-dimensional distributions of sediment EEA with fewer artifacts than traditional techniques. The output of this planar sensor reveals real-time proteolytic enzyme activity patterns at high resolutions (approximately 50 to 100 μm pixel size). Substantial heterogeneity and millimeter scale "hot spots" of EEA have been observed using this sensor system. In the present study, this 2-D enzyme sensor system was used to investigate seasonal EEA patterns of leucine aminopeptidase at two subtidal muddy sediment sites in Great Peconic Bay, an estuarine environment on the eastern end of Long Island, New York. EEAs (aminopeptidase, β-glucosidase, and phosphatase) were also measured by traditional incubation techniques for comparison. The underlying hypothesis was that EEA distributions would track seasonal patterns of temperature (general metabolic activity), substrate supply (nutrient remineralization rates), and macrofaunal activity (particle reworking patterns); measurements of which were made at the same sites and time.

2. Materials and Methods

a. Study site and sampling

Sediment samples were collected seasonally at two sites in Great Peconic Bay (Fig. 1) during 7 cruises spanning the period from spring 2009 to fall 2010. Great Peconic Bay is part of the Peconic estuary system, which is situated between the North and South Fork at the east end of Long Island, NY (USA). It is a shallow (less than 9 m), well-mixed tidal estuarine basin with little or no seasonal stratification. Circulation is dominated by tidal effects that are much greater than freshwater inputs. Salinities are in the range of 25 to 28 and temperature varies seasonally from −1 to 28°C. Site 1 (40°56.055'N, 72°29.887'W) is located at the center of the Bay and had a water depth of approximately 7 m. Site 2 (40°57.298'N, 72°29.983'W) is to the north of Site 1 and had the same water depth (approximately 7 m). Both sites are characterized by fine grain muddy bottoms (Katuna, 1974). Samples from Sites 1 and 2 were collected seasonally during the period from July 2009 to June 2010. Sediment samples were collected using acrylic box corers (30 × 12.5 × 30 cm) by scuba divers. Cores were stored in containers filled with unfiltered sea water from the sampling site, both on board and during transportation to the laboratory. After reaching the laboratory, cores were immediately stored in a cold room at in situ temperature. EEA analysis and supporting measurements were conducted within 24 hours after sampling. Pore water depth profiles of NH_4^+, NO_3^-, ΣCO_2, and PO_4^{3-} were measured and anoxic incubations were set up in the laboratory to estimate respective solute production or consumption rates within 24 hours of sampling. Sediment bacterial abundances were documented during two seasons (fall 2009 and winter 2009 to 2010) at both sites.

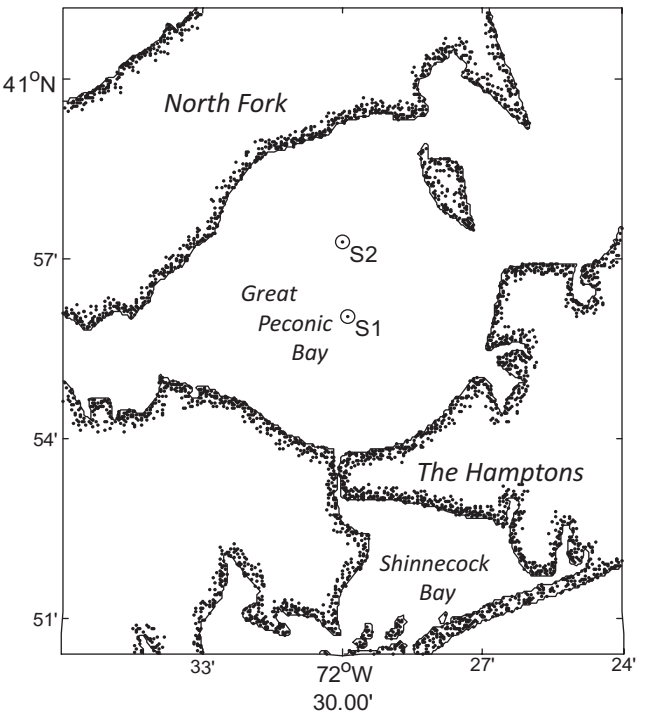

Figure 1. Location of sampling sites in Great Peconic Bay, at the eastern end of Long Island in New York.

b. Pore water analyses and bacteria counts

Sediment cores were sectioned rapidly at 1- to 3-cm vertical intervals. The sampled intervals were transferred with minimal exposure to air (seconds) into centrifuge bottles continuously purged with N_2. The sediment was centrifuged under N_2 at 4,500 rpm for 20 minutes at the temperature of collection and the supernatant pore water was sucked into syringes (no gas head space) and filtered through 0.2 μm polysulfone inline filters. We have found this procedure, when carried out rapidly, to produce analytical results indistinguishable from cores handled exclusively within a N_2-filled glove bag. Pore water was analyzed for ΣCO_2 within 24 hours of collection by the flow injection analysis with conductivity detection (Aller and Mackin, 1989; Hall and Aller, 1992) . Pore water samples for NH_4^+ and NO_3^- analyses were frozen immediately after filtering, and samples for reactive PO_4^{3-} analysis were acidified before further analysis. Nutrients were measured using colorimetric methods modified for a 96-well microplate reader: NH_4^+ (Solorzano, 1969), NO_3^-/NO_2^- (Doane and Horwath, 2003; Miranda et al., 2001), and PO_4^{3-} (Presley, 1971). Sediment porosity was estimated from differences between wet and dry weights assuming a solid phase density of 2.6 g cm^{-3}. Production estimates for ΣCO_2 and NH_4^+ were derived from serial anoxic incubations of 18 cm long whole cores that were incubated in sealed glass

tubes and kept in oxygen-free, impermeable bags over 1 to 4 weeks (Aller and Mackin, 1989; Waugh et al., in prep.). Epifluorescence direct counts of bacteria were made following staining with acridine orange after Hobbie and colleagues (1977) and Watson and colleauges (1977).

c. EEA measured by traditional incubation methods

The activities of three extracellular enzymes were measured in homogenized intervals of sediment: β-glucosidase (BG), leucine-aminopeptidase (LAP), and phosphatase (PA), corresponding to the decomposition of organic C, N, P substrates respectively. The procedure of Hoppe (1983) was generally followed with minor modifications (Aller and Aller, 1998). Briefly, sediment cores were sub-cored using a small butyrate tube (O.D. = 7.5 cm). The sub-cored sediment was extruded and sliced at 0.5 to 2 cm intervals, with thinner intervals near the top of the core. Sediment layers were quickly transferred into 50-ml centrifuge tubes filled with N_2 gas. Tubes were then transferred to a N_2 filled anaerobic chamber, where the sediment in each tube was well mixed by hand, and after which about 0.6 g of sediment was transferred into 15-ml centrifuge tubes. The sediment in each 15-ml centrifuge tube was slurried by adding 5.0 ml of 0.2 μm pore size filtered deoxygenated sea water. Specific fluorogenic substrates were then added, and the tubes were incubated for one hour with continuous shaking in the dark at the temperatures of core collection (absolute temperature approximately 0 to 24 °C). The extracellular enzyme kinetic parameters (V_{max} and K_m) were measured in two summer seasons that had relatively high activity levels. The final concentration of each fluorogenic substrate that was added to slurries was determined based on V_{max} and K_m, respectively. The final concentrations of each substrate were: L-leucine 7-amido-4-methylcoumarin hydrochloride (Leu-MCA) 1.6 mM, 4-methylumbelliferyl glucoside (MUF-G) 1.0 mM, and 4-methylumbelliferyl phosphate (MUF-P) 1.8 mM. Incubations were stopped by adding 5.0 ml pH 10.5 glycine buffer for MUF-based substrates or 5.0 ml of 30% acetone for MCA-based substrates (Belanger et al., 1997). Mixtures were then centrifuged at 4,500 rpm for 15 min, and the supernatants were filtered through 0.2 μm pore size polysulfone filters. Fluorescence was measured at 450 nm (with excitation at 365 nm) for MUF or at 440 nm (with excitation at 360 nm) for MCA using a Hitachi F-4500 fluorescence spectrophotometer. All samples were measured in duplicate, and one control (boiled sediment) was also incubated to correct for background fluorescence and for abiotic cleavage of the artificial substrates. Potential background interference by organic detritus in sediment as discussed by Arnosti (2011) was found to be negligible after filtration. Control measurements showed very low fluorescent signals at all times for BG and LAP. For PA, however, substrate MUF-P was found to undergo slow but steady hydrolysis even in enzyme deactivated sediment (boiled or microwaved). To our knowledge, no similar phenomenon has been reported previously, and the exact mechanism that causes such abiotic hydrolysis remains unclear, but it is certainly worthy of attention for those utilizing MUF-P in sediment. In our current study, fluorescence signals from MUF-P were corrected by subtraction of background rates measured in boiled sediment controls.

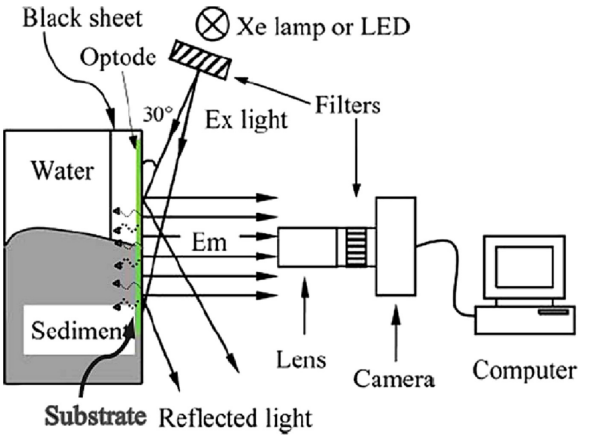

Figure 2. Imaging instrumentation used for two-dimensional leucine-aminopeptidase measurements (modified after Zhu et al., 2005). The position of the enzyme substrate against the sediment is shown in green.

d. EEA controlled-release foil sensing system

Our planar sensing system is based on the controlled release of a fluorogenic substrate from a thin hydrogel membrane (hydromed D4) into a contacting sediment interface, while the resulting fluorescence generated by enzyme hydrolysis is monitored over time. The sensor foils, which in this application utilize Leu-MCA as substrate, reveal in situ, real-time proteolytic enzyme (leucine-aminopeptidase) activity patterns across the planar surface at high spatial resolution (approximately 50 to 100 μm pixel size). Leu-MCA was chosen because of the importance of proteolytic enzymes in organic matter decomposition and because the fluorescence response of the fluorophore MCA is independent of pH within the range normally expected in marine sediments. Because the sensor foils are transparent, enzyme activity patterns can be related directly to visible physical and biological structures in bioturbated sediments, optimizing our ability to interpret the relationship of bacterial activities to sedimentary structure. Details about membrane preparation and performance are described in Cao et al. (2011).

e. Instrumentation and deployment

A schematic drawing of the optical system for 2-D Leucine-Aminopeptidase (LAP) activity measurements is shown in Figure 2. The sensor membrane is deployed in a manner similar to other planar sensors: a thin foil with the enzyme substrate inserted vertically several centimeters (usually approximately 10 cm) into sediment or placed horizontally onto a sediment surface. In both cases, images were taken perpendicular to the plane of the sensor foil. A companion foil that is prepared the same way as the sensor foil but which releases MCA instead of substrate (Leu-MCA), was used to correct for diffusive loss of the

Table 1. Depth-integrated nutrient inventories and production rates in different seasons over 0 to 15 cm.

	Temperature (°C)		NH_4^+ (mmol m^{-2})		PO_4^{3-} (mmol m^{-2})		ΣCO_2 Production (mmol m^{-2} d^{-1})		NH_4^+ Production (mmol m^{-2} d^{-1})	
Seasons	Site 1	Site 2	Site 1	Site 2	Site 1	Site 2	Site 1	Site 2	Site 1	Site 2
Summer 2009	22.3	23.7	5.3	8.0	1.4	2.6	16.6	18.8	1.8	6.4
Fall 2009	17.5	11.1	15.9	8.9	1.0	1.9	8.7	4.2	0.2	0.5
Winter 2010	−0.29	3.4	3.03	7.4	0.7	1.3	1.2	3.3	0.2	0.2
Spring 2010	15.1	22.1	4.9	5.2	3.8	2.3	10.1	37.7	1.8	6.7

fluorescence signal out of the image plane (Cao et al., 2011). Images were obtained with a theoretical pixel resolution of 50 × 50 μm. To further avoid reflected light, the fluorescence image was recorded with excitation light at an angle of incidence of approximately 30° and emission at 90° to the target plane. Images were taken at one minute intervals over a 45 to 90 minute period. Captured images were analyzed with Image-Pro Plus (version 4.1) and Matlab (version 7.0.4). More details about sensor deployment and calculations are described elsewhere (Cao et al., 2011).

3. Results

a. Nutrients and environmental parameters

Depth-integrated nutrient inventories over the top 15 cm as well as depth-integrated production rates of ΣCO_2 and NH_4^+ at each season for both sampling sites, are shown in Table 1 (detailed data from Waugh et al., in preparation). NO_3- concentrations in pore water and overlying water did not exceed 5 μM, and they are not considered further here. The net NH_4^+ production rates measured with incubations were corrected for reversible adsorption assuming an adsorption coefficient of 1.3 (Mackin and Aller, 1984). Nutrient concentrations are of the same magnitude at the two sampling sites and have similar patterns of seasonal variation. For both sites, lower nutrient concentrations occurred in winter and higher concentrations in summer and fall. Dissolved nitrogen-phosphorous (N/P) ratios ranged from 1.7 to 16.3, lower than the canonical Redfield ratio of 16/1 in most seasons (assuming quasi-steady state at each sampling time). Ratios of N/P were lower in summer and spring for both sites (1.6 to 3.2), compared with significantly higher ratios (5.1 to 16.3) in fall and winter. Production rates of ΣCO_2 and NH_4^+ showed that organic carbon and nitrogen decomposition rates varied seasonally. Production rates were over five times higher in spring and summer than in fall and winter.

b. Seasonal patterns of EEA

Activities of three extracellular enzymes β-glucosidase (BG), leucine aminopeptidase (LAP), and phosphatase (PA) were measured by traditional incubation techniques (slurries).

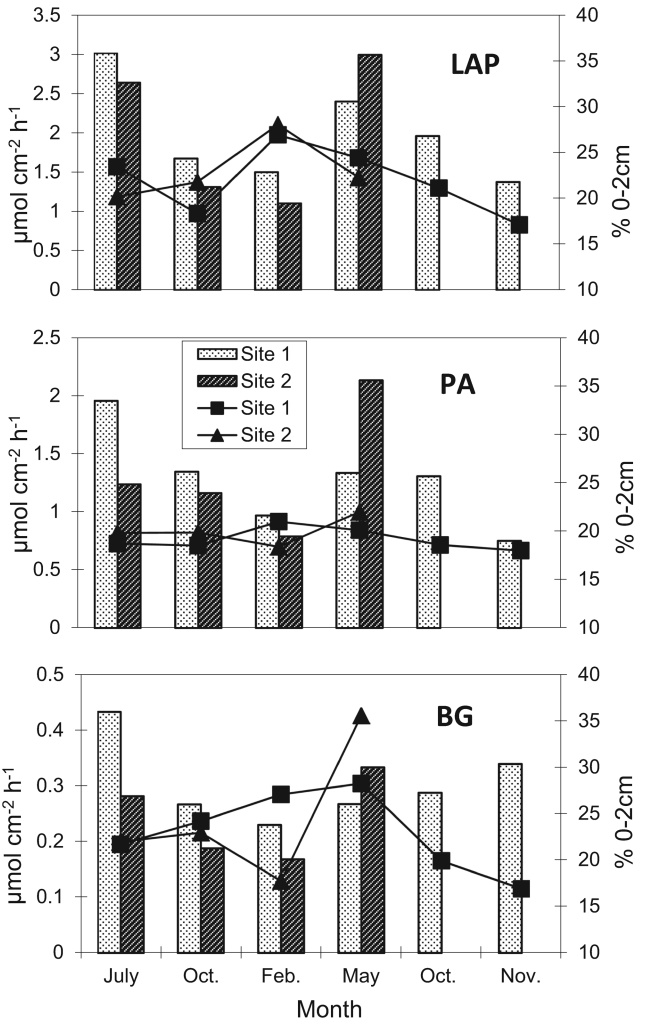

Figure 3. Vertically integrated activities (as bars; traditional methods) over the top 12 cm of leucine aminopeptidase (LAP; top), phosphatase (PA; center), and β-glucosidase (BG; bottom) in different sampling seasons from July 2009 through November 2010, overlaid by the percentage of extracellular enzyme activities in the top 2 cm for depth integrated values (filled symbols). While LAP activity overall was greater than PA activity which was followed by BG activity, all three enzymes showed similar seasonal patterns activities with lowest values in winter, highest in the summer and Site 1 more active than Site 2.

Vertically-integrated activities (0 to 12 cm) are shown as bar graphs in Figure 3. Also plotted is the percentage of EEA in the top 2 cm for depth-integrated values. The relative magnitudes of activities of the three enzymes is LAP>PA>BG, consistent with most previous studies of coastal sediment EEA (Poremba and Hoppe, 1995). All three enzymes showed similar

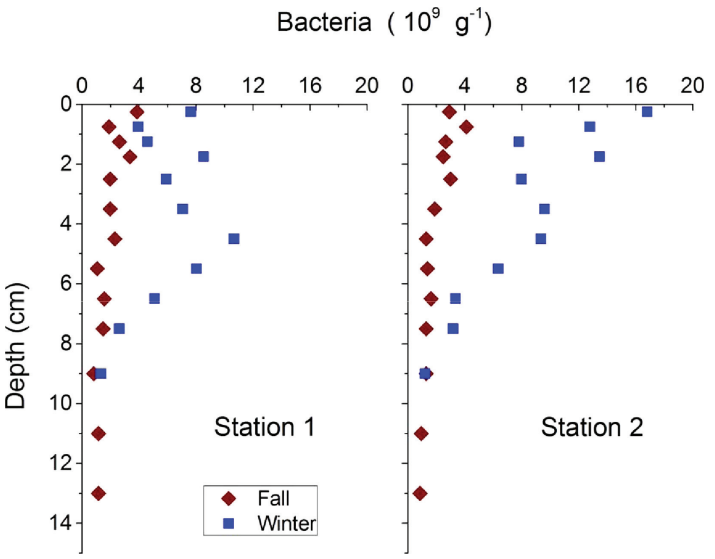

Figure 4. Comparison of bacterial abundances during fall and winter 2009 at Sites 1 and 2. In winter, both sites had higher concentrations of bacteria in the approximate upper 8 cm.

seasonal patterns with EEA lowest in winter, beginning to increase during early spring, peaking in summer, and then gradually decreasing. Site 1 had higher enzyme activities than Site 2 among all series except in May 2010, when EEA of all three enzymes was higher at Site 2. BG had a higher proportion of its activity in the top 2 cm of sediment than the other two enzymes.

c. Bacterial abundance

Bacterial abundances were several times higher in winter than in the fall, in spite of much lower nutrient concentrations, decomposition rates, and EEA during that season (Fig. 4, Table 1). While bacterial cell abundances generally decreased with increased depth in the sediment, in winter a subsurface (3 to 6 cm) maximum region was found at both sites.

d. 2-D enzyme activity distribution patterns

Seasonal enzyme activity distributions of surface sediment at Site 1 are shown in Figure 5. Enzyme activities in individual pixels were converted to pseudo–colored images which readily show both horizontal and vertical heterogeneities of enzyme activities.

A clear seasonal variation can be observed in the LAP profiles at Site 1, between April 2009 and May 2010 (Fig. 5). Late spring and summer (May to July) had much higher overall EEA than fall to winter and early spring at all depths. In April 2009, maximum values were

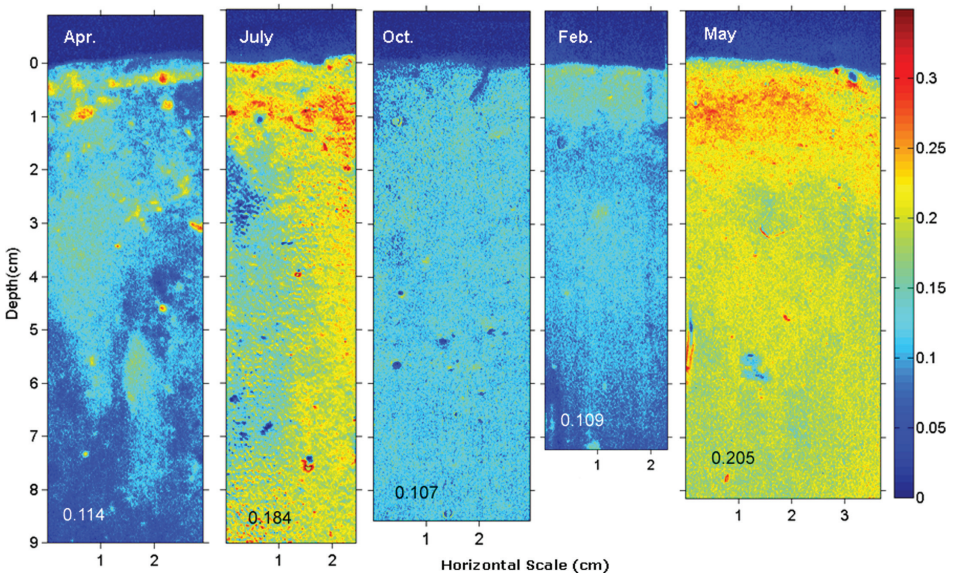

Figure 5. Two-dimensional extracellular leucine aminopeptidase (LAP) distribution patterns plotted as pseudo-colored images in cores collected in different seasons of Site 1. From left to right: April 2009, July 2009, October 2009, February 2010, and May 2010. The x- and y-axes are actual length scales within the sediment. Point 0 on the y-axis indicates the position of the water-sediment interface. Because the sediment surface is seldom level, the exact position of the interface is estimated. The colored bar reflects extracellular enzyme activities (μmol g-wet^{-1} h^{-1}). The average extracellular enzyme activity over the image area is indicated at the lower left in each panel.

generally found between 0.5 to 1 cm depths. A relatively continuous layer with high values was apparent at around 0.5 cm depth, and isolated microzones of elevated activity, termed hot spots, were found at about 1 cm depth. The activities decreased rapidly with depth and showed less horizontal heterogeneity in deeper sediment layers. EEA was generally higher at all sampled depths in July than in April, although the zone of maximum activity still occurred within the top 2 cm. Fluorescence signals on the left bottom part of the sensor foil were blocked by sediment particles accidently penetrating the space between the membrane and core wall, and this area was excluded from calculations. In the fall, the overall EEA magnitudes were comparable with those in April, however, the spatial distribution was quite different. The 2-D EEA image in the fall (October) lacks a downward gradient and thus showed more vertical homogeneity. The surface EEA in the fall was lower than in April, while EEA in deeper sediment was higher than in April. From fall to late winter, vertical gradients became more distinctive as the EEA at the sediment surface increased and the EEA in the deeper regions decreased. The maximum EEA in surface sediment during February corresponded to deposition of planktonic debris from the late winter to spring bloom. From winter to late spring (Feb to May), EEA gradually increased throughout approximately the

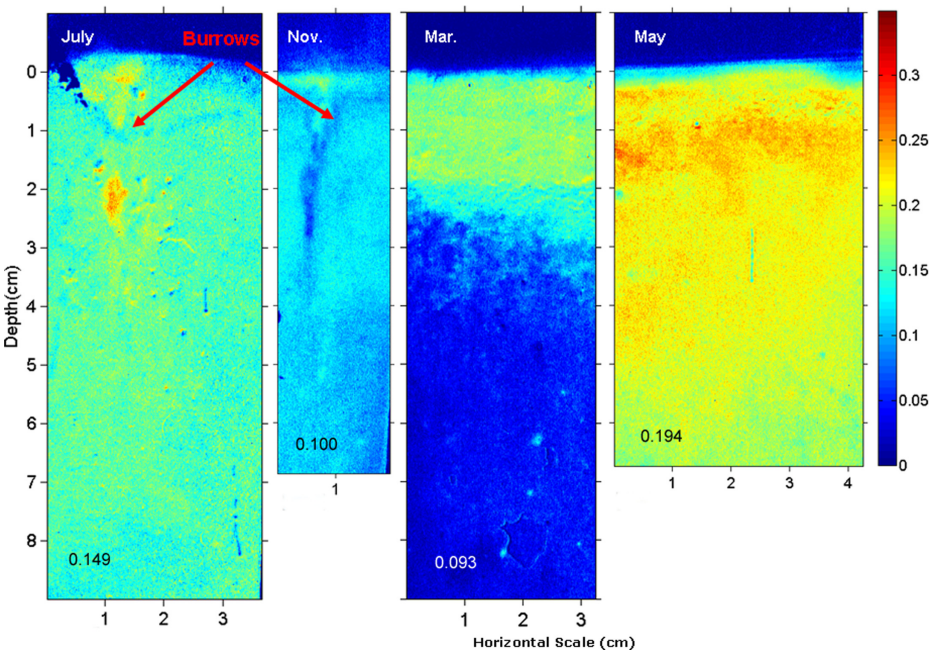

Figure 6. Two-dimensional extracellular leucine aminopeptidase (LAP) distribution patterns plotted as pseudo—colored images in cores collected in different seasons of Site 2. From left to right: July 2009, November 2009, March 2010, and May 2010. Point 0 on the y-axis indicates the position of the water-sediment interface. The colored bar reflects extracellular enzyme activities (μmol g-wet^{-1} h^{-1}). The average extracellular enzyme activity over the image area is indicated at the lower left in each panel.

upper 10 cm of the deposit. The EEA in deeper sediment during May was much higher than that at the same depth in February, though much lower than that in surface maximum zone.

Seasonal enzyme activity distributions at Site 2 are shown in Figure 6. Generally Sites 1 and 2 showed similar seasonal EEA distribution patterns. In addition, two burrow structures were captured in summer and fall samples at Site 2. EEA was low in the water-filled burrow centers but was enhanced in immediately surrounding sediment. An early spring bloom occurred during late winter sampling (March). Phytoplankton detritus deposited from the late winter to spring bloom formed a fluffy layer with a thickness of approximately 2 cm on surface sediment. EEA was greatly enhanced in this layer. Below the fluff layer, EEA remained at the low activity more typical of winter. The EEA profile in May at Site 2 was similar to that at Site 1, with a difference in the position of the maximum EEA layer. Site 1 had the highest EEA at the very surface; while at Site 2, an activity maximum occurred within a subsurface layer at 1 to 2 cm.

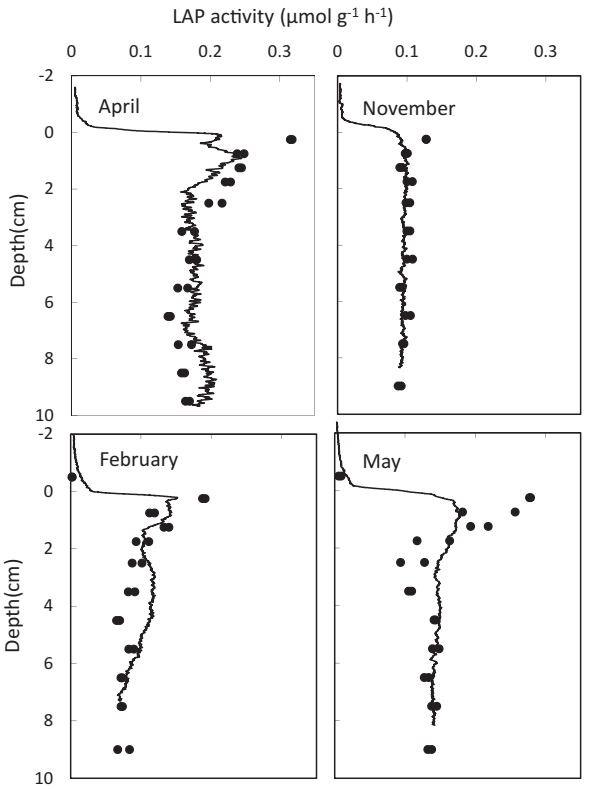

Figure 7. Vertical profiles of horizontally averaged enzyme activity obtained from 2-D sensor images (black line) compared to results from traditional incubations (black circles).

4. Discussion

a. Comparison of enzyme activity profiles determined by fluorosensor and traditional incubations

The EEA distributions obtained by 2-D planar imaging can be compared with EEA determined using traditional techniques by horizontally averaging the 2-D images to derive equivalent vertical EEA profiles. Vertical profiles derived from the two techniques showed similar general features with maximum EEA at or just below the sediment surface and a decrease with depth during most seasons (Fig. 7, four Site 1 measurements shown). However, profiles from traditional incubations have relatively higher activity at the sediment surface as well as sharper downward gradients. While such differences may come from natural heterogeneities between cores, the consistency in the relative differences implies methodological artifacts in one or both techniques.

We believe that the most likely explanation for these differences is the manipulation of sediment during the traditional EEA method. The traditional method involves slicing sediment cores, followed by slurrying and serial incubation of the slurry. Both steps may introduce EEA artifacts. When slicing sediment cores, the process of drawing off overlying water to expose the sediment surface typically causes a small degree of dewatering and compaction of the uppermost sediment layer, which could result in an overestimation of the per wet weight sediment EEA. When sediment is slurried, additional pore water is added and the combined material well mixed. During slurrying the microstructure of the sediment is largely destroyed, the porosity is increased, and tortuosity decreased. The adsorption and diffusion behaviors of both EE and availability of enzyme substrate are thus changed, which increases the chances of EE meeting a target substrate molecule (Arnosti, 1995). Considering the relative enhanced and reactive organic matter content and elevated bacteria abundance in surface sediments (Fig. 4), the manipulations may result in overestimation of EEA relative to undisturbed sediment structure (e.g., Hansen et al., 2000).

b. Annual pattern of EEA in Great Peconic Bay

As far as we are aware, this study is the first to examine seasonal 2-D EEA distributions in sediments, and dynamic coastal deposits in particular. The results demonstrate significant seasonal variations in both the average magnitude of EEA and its distribution in surface sediment. Vertically averaged EEA (over the upper 12 cm) has the lowest values in fall and winter (approximately 0.09 to 0.1 μmol g-wet^{-1} h^{-1}). The deposition of spring bloom detritus during late winter to spring results in enhanced EEA focused into the surface most sediment layer. As temperature rises and reactive substrates penetrate into deeper layers by biogenic reworking, average EEA (0 to 12 cm) increases and reaches an annual maximum during summer (0.15 to 0.2 μmol g-wet^{-1} h^{-1}). The activity subsequently decreases again during fall (Figs. 5, 6).

Distributions of EEA in surface sediment also showed significant seasonal patterns. During winter and early spring, infauna are depleted in number and relatively inactive. During these seasons, the surface sediment showed generally less lateral heterogeneity in EEA. In summer and fall, however, enhanced heterogeneity at multiple spatial scales was observed mostly due to elevated particle reworking and bioirrigation by benthic fauna. A sharp contrast is apparent in EEA profiles between spring and fall (Fig. 5; Apr., Oct.). The two seasons have comparable averaged EEA magnitudes, but the distributions are different. In spring, primary production increases rapidly resulting in pulsed deposition of reactive organic matter (OM) and stimulation of bacterial activity at the sediment surface; however, the activity of the benthic fauna clearly lags the deposition of the bloom detritus as illustrated by the presence of a distinct layer. The late winter EEA showed obvious decreases with depth (an almost two layer structure) but not much horizontal heterogeneity. In fall, the primary production drops (Lonsdale et al., 2006), causing decreased OM supply relative to summer. However, the benthic fauna are still highly active, reworking and irrigating sediment,

forming burrow structures and redistributing organic matter that brings reactive substrate into deeper layers.

Bacterial abundances appear to respond to similar seasonal forcing. In the fall, when benthic fauna are extremely active and the organic matter supply drops significantly compared to summer (as reflected by lower EEA and nutrient and CO_2 production rates), the net production of bacteria may be limited and abundances correspondingly low. In late winter (February), bioturbation is minimal, lowering grazing pressure. At the same time, the spring phytoplankton bloom results in the introduction of labile organic substrates to the seabed. The net growth of bacteria is almost certainly stimulated as a consequence, resulting in densities several times higher than in the fall and producing a clear surface maximum. Although this seasonal abundance pattern has not been documented in other studies to our knowledge, our interpretations are consistent with processes in Peconic deposits.

c. Surface sediment heterogeneity and decomposition "hot spots" discriminated by EEA imaging

The 2-D EEA sensor allows the discrimination of small-scale heterogeneities, which appeared to be common during certain seasons. Previous studies applying 2-D optical sensors in surface sediment have also revealed various scales of heterogeneity. For example, CO_2 patterns reflect macrofaunal burrow structures at the millimeter to centimeter scale (Zhu et al., 2006), and O_2 images exhibit microsites of preferential consumption, that is, hot spots of remineralization activity (Glud, 2008).

The information derived from the EEA sensor system differs from other optical sensors such as O_2, pH, or pCO_2 planar sensors, in that, firstly, it directly measures reaction rates in contrast to concentrations. Secondly, as shown by previous studies, EEA is dominantly associated with solid particles and is not directly subject to solute transport processes such as molecular diffusion and bioirrigation (Arnosti, 2011; Cao et al., 2011). Thus, EEA imaging directly and uniquely reflects biosubstrate properties of sediment particles, including the size, density and saturated enzyme activity level of reactive organic aggregates. EEA imaging also reveals reaction heterogeneity under completely anoxic in addition to oxic conditions, which is not possible for O_2 sensors.

These specific properties can cause EEA images to look different from 2-D patterns obtained by pH or pCO_2 fluorescence sensors (Zhu et al., 2005; Zhu et al., 2006). One of the most obvious differences is that most 2-D EEA distributions (Figs. 5, 6) showed a granular pattern at the millimeter scale rather than the relatively smooth patterns obtained by the solute concentration sensors at micrometer scales. Conversion of solute concentration gradients such as H^+ (pH) into net reaction rates can also produce more granular patterns but unlike the more direct EEA measurements these may be due in part to calculation artifacts (noise amplification) (Zhu et al., 2006). In spite of the recognition and ubiquity of heterogeneity associated with organic aggregates in sediments, the significance of aggregates during early diagenesis has not been well studied, particularly under anoxic

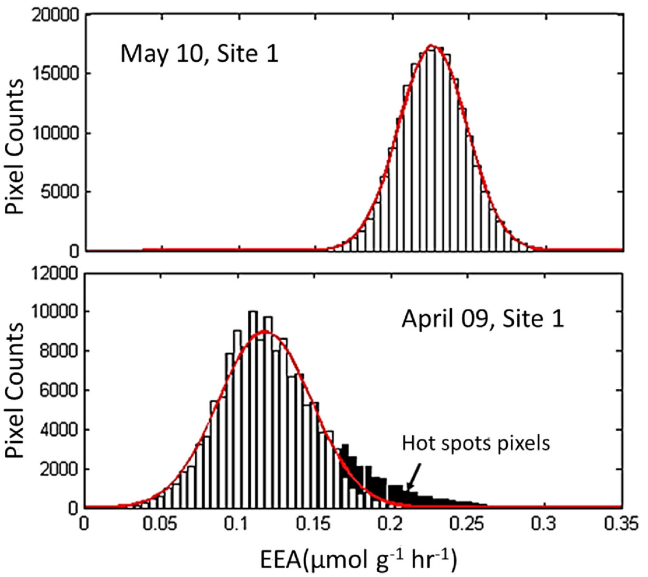

Figure 8. Histograms showing surface sediment (0–2 cm) extracellular enzyme activity (EEA) distributions without (top) and with (bottom) hot spots. The x-axis is the range of extracellular enzyme activities and the y-axis represents the number of pixels that are within each extracellular enzyme activity interval. Red lines in each figure are normal distribution simulations based on sample mean and variance.

conditions where O_2 sensors do not reveal reactivity patterns (Jorgensen, 1977). We examined the effect of microniche heterogeneity on local statistical distributions of EEA during different seasons. In most seasons, when EEA data of all pixels from a specified depth interval (Fig. 8, top) are plotted as a histogram, the resulting distribution shows a typical symmetrical, normal distribution pattern, with a skewness of −0.03. This symmetry suggests that aggregates and reactive substrate are relatively uniformly mixed by physical and chemical processes. In those seasons, although there are microsites of high EEA levels, they appear randomly and approximately normally distributed about a mean value and are compensated by equivalent sites of low EEA.

There are seasons and zones within the sediment, however, where relatively high EEA microniches are larger, thus distinctly skewing EEA distributions in a non-random fashion. For example, when EEA data from the top 2 cm of Site 1 in spring 2009 were plotted (Fig. 8 bottom), the distribution is not symmetrical but skewed to higher values (white and black bar), with a skewness of 0.77. This skewed distribution implies that additional highly reactive organic sources were introduced. These additional high EEA spots are a distinct departure from a symmetrical random distribution. The comparison between these two samples also shows higher relative standard deviation (RSD%) in EEA distributions

during April than in May (34.7% versus 10.1%), consistent with these differences in the distribution patterns.

It is clear that the micro-scale distribution of EEA can change seasonally and that distinct microniches of elevated activity are more or less obvious. How then are such phenomena best defined and quantified? We identified microniches by both size and relative activity. First, we set an EEA threshold of 1.34 times the mean value within a depth interval (that is, where EEA positively exceeded 1 standard deviation). Second, the imaged area of the enhanced EEA pixel group had to exceed 1 mm^2 in order to differentiate the region from the regular background EEA grain scale. In the case of the April distributions, hot spots defined in this manner contributed 9.9% of the image area and contributed 15.7% of overall EEA activity (black regions, Fig. 8 bottom). If these hot spots are excluded from the distribution, the skewness drops to 0.27 (white bar), indicating a more symmetrical distribution compared to May. It should be pointed out that the contribution of functional hot spots in this example may be underestimated. The positive value of skewness (0.27) after hot spot subtraction may be a sign of this underestimation.

Based on these definitions, three sediment samples were found to have zones of significant hot spots accounting for a substantial portion of total decomposition activity. Two of these cases were in regions surrounding burrow structures; the other is the previously discussed example which we believe reflects initial stages of the penetration and mixing of phytoplankton debris into the deposit following the spring bloom.

d. Hot spots associated with burrow structures

Benthic fauna significantly change surface sediment structure. Through processes including particle manipulation, grazing, excretion/secretion, nutrient release, irrigation, and particle transport, macrobenthos greatly influence pathways, rates, and extents of organic matter remineralization and associated reactions, causing a more complex transport of particles (sediment reworking) and fluids (bioirrigation), and create a three dimensional zonation pattern of geochemical processes (Aller, 2001; Bertics and Ziebis, 2009; Glud, 2008; Kristensen and Kostka, 2005; Volkenborn et al., 2012). Furthermore, abandoned tubes or burrows are found often surprisingly stable and can last for months to years after being vacated, acting as traps for labile organic material (Aller and Aller, 1986; Zhu et al., 2006). Previous studies have shown elevated EEA activities around both recently infilled as well as actively irrigated macrofaunal burrows (Aller and Aller, 1998; Boetius, 1995; Wenzhofer and Glud, 2004). In the present study, we also found elevated EEA associated with burrows (Fig. 6; July, November), but regions of enhanced EEA were characterized by relatively abundant hot spots rather than continuously elevated EEA distributions. These patterns may reflect burrow properties of particular species or may be a more accurate general indication of enhanced EEA around burrows. Fecal material and excretion of mucus may also promote the formation of hot spots. In any case, there are insufficient data on in situ burrow structures at this point to determine the possible generality of the distributions.

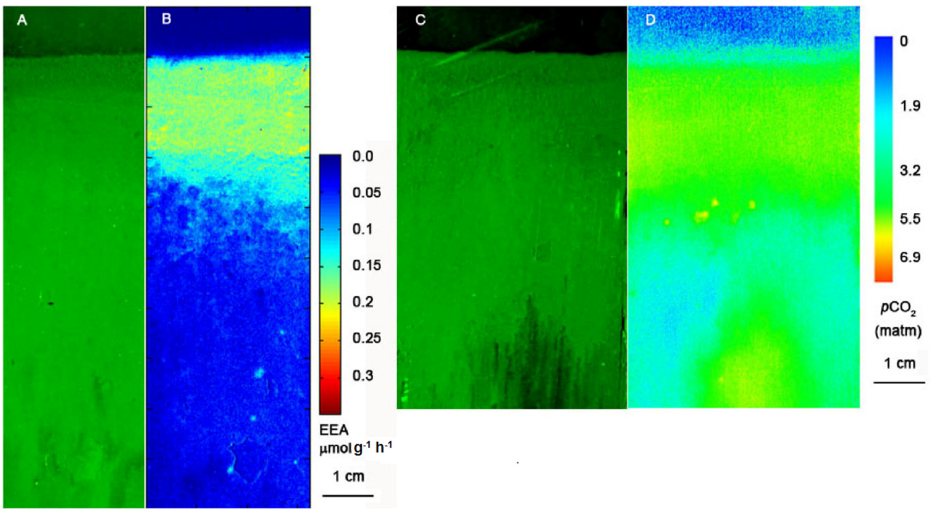

Figure 9. Vertical sections from two cores taken during the spring bloom (late Feb–Mar 2010) in Great Peconic Bay at Site 1. (a, c) Raw visible images under green light corresponding to each sensor image (Fe-sulfide is black). (b) Aminopeptidase activity (LAP). (d) pCO_2 concentration. Note that the vertical and horizontal scales are in centimeters (scale bar). The depositional focusing of reactive particles and the relative lack of bioirrigation results in the close correspondence of reactive particle and metabolite distributions near the sediment-water interface.

e. Impacts of algal blooms and pulse deposition of detritus

Site 2 sediment collected in March 2010 had a fluff layer with a thickness of approximately 2 cm at the surface (Figs. 6, 9). This fluff layer largely consisted of phytoplankton detritus deposited from an early spring bloom that presumably occurred a few days to weeks before sampling. A clear boundary can be found between the fluff layer and deeper sediments. Within this layer, LAP activity reached an abnormally high level for that season. The average value even exceeded the surface EEA in summer. Below this fluffy layer, however, EEA remained at the low activity more typical for winter. The integrity and distinctive nature of the surface fluff layer shows that surface sediment had not yet been reworked or extensively irrigated by benthos. The lack of substrate dispersion from particle bioturbation and minimal bioirrigation, resulted in a close correspondence between EEA and remineralized metabolites, as demonstrated by pCO_2 patterns obtained at the same site (more details about the principle and deployment of the pCO_2 sensor can be found in Zhu and Aller (2010). High pCO_2 was clearly superimposed with high EEA in the fluff layer (Fig. 9). This superposition demonstrates that EEA directly reflects metabolic activity during this sampling period. As discussed previously, as biogenic transport processes such as bioirrigation become more intense in the summer and fall, and reactive substrates penetrate and are dispersed into the deposit, solute concentrations and metabolite build up patterns may not readily reflect local remineralization activity. Another very interesting fact is that in

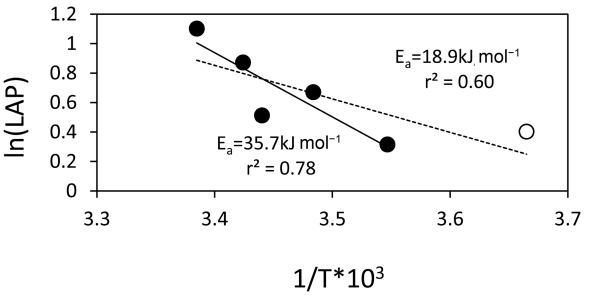

Figure 10. Natural log of depth integrated extracellular enzyme activities for Site 1 samples collected in different seasons plotted against 1/T, where T is absolute temperature. The hollow circle is the extracellular enzyme activity from February 2010 while the filled circles are extracellular enzyme activities from July 2009, October 2009, May 2010, October 2010, and November 2010. The solid line is a linear regression of the solid circles and the dashed line is the regression of all points.

contrast with the highly elevated aminopeptidase activity in the surface-most fluff layer, the glucosidase activity within the top 2 cm layer remained low (Fig. 3). Such decoupling between GA and LAP is a good example of the regulated response of bacteria to the characteristics or the "quality" of the polymeric organic material pool. While directly bioavailable carbohydrate monomers may be abundant in the fresh phytoplankton debris layer as a result of cell lysis, bacteria tend not to expend much energy on gluocosidase excretion but rather on stimulating proteinase excretions to satisfy their nitrogen demands.

The EEA distributions from late winter and spring to late spring in Great Peconic Bay provide an illustration of the non-steady state seasonal remineralization processes previously documented in estuarine surface sediments (Breuer et al., 1999; Bruno et al., 1980; Gerino et al., 1998; Graf, 1992; Hunt, 1983). As spring bloom material is deposited on the seabed and reworked into the underlying deposit by meio- and macroinfauna, microniche hot spots develop as seen in our April samples. The low temperatures and relatively low infaunal activity at the time both hinder complete decomposition and enhance temporary preservation of phytoplankton detritus.

f. Factors controlling EEA in Great Peconic Bay sediments

Our results show that sedimentary EEA activity varies significantly with the seasons due in part to temperature and in part to substrate availability (Figs. 4–6, 10). At a fixed substrate composition, the temperature dependence of LAP in slurried sediment follows an Arrhenius rate law with an apparent activation energy (E_a) of approximately 30.6 kJ mol^{-1} (Cao et al., in preparation). When the natural log of the depth-integrated EEAs (12 cm) measured in Site 1 cores by traditional (slurried) methods is plotted versus 1/T (T = absolute temperature at collection), the apparent activation energy derived from the slopes is much smaller: 18.9 kJ mol^{-1} (Fig. 10, all points included). However, if the EEA value obtained during the

winter to spring transition is removed from the regression, the apparent activation energy is approximately 35.7 kJ mol^{-1} (Fig. 10, open circle excluded), and is more comparable to independent experimental measurements (also slurried). The fit of depth-integrated EEA from different seasons in the E_a curve demonstrated that temperature accounted for most of the annual variation in sediment EEA. In other words, after normalizing EEA for each season to the temperature, potential EEA inventory is stable during most of the year. This phenomenon implies that high molecular weight organic matter hydrolysis is a rapid process in Peconic Bay surface sediments rather than being a limiting step in OC remineralization. The inventory level of LAP (0 to 12 cm) present is sufficient to accommodate the range of variation in substrate supply over most of the year. However, during the spring bloom period (February to March) labile substrate deposition enhances EEA above that expected from variation in T alone and lowers the estimated E_a derived from a simple plot of all EEA measurements versus 1/T over the annual period. The mechanism for net enhancement of EEA is presumably either stimulated LAP synthesis or a shift of dominant LAP to a low E_a isoenzyme or both.

The activities of the three measured classes of enzymes correlated with each other, suggesting coupled controlling factors (Fig. 11). When EEAs versus their respective end member nutrient product concentrations were plotted (LAP versus DIN, BG versus. ΣCO_2, and PA versus PO_4^{3-}) among all seasons from all depth intervals, no significant relationships were found (data not shown). In contrast, EEA and direct measurements of metabolite production such as depth-integrated NH_4^+ and ΣCO_2 production rates, clearly correlate (Figs. 12a, b). The correlations between EEA and respiration rates reflect their mutual dependence on the availability of labile substrates and temperature; however, the EEA cannot be directly converted into realized remineralization rates (e.g., ammonification rates) because the enzyme activities are the saturated kinetic values and because the efficiency of cell uptake of EEA products is unknown. Relative to the potential EEA rates the apparent overall conversion efficiencies to net remineralization could be as low as a few percent (e.g., Fig. 12b). Previous studies have found inorganic phosphate is the dominant regulating factor of phosphatase activity (Hoppe, 2003). However, the pattern is not obvious in this study, probably because bacteria may also produce PA targeting the organic part of phosphate containing polymers, rather than phosphate requirements per se, especially in carbon-limited subsurface sediments (Hoppe and Ullrich, 1999).

Even though the suite of EEA in Great Peconic Bay seems to be co-regulated in general, the ratios between enzymes may still reflect a nutrient limitation regime shift among seasons. It has been suggested that the EEA ratios between enzyme groups can be potential nutrient limitation indicators (Hill et al., 2010). In this study, when enzyme ratios (LAP/PA) were plotted against ratios of inorganic nutrients (N/P derived from inventories 0 to 15 cm) (Fig. 12c), we found that during warm seasons (April to mid October), the N/P ratio was low compared with that in cold seasons (late Oct to March). In these two periods, no clear relationship was found between LAP/PA and N/P. In the cold seasons, the N/P was much higher, presumably due to lower biological activity and relatively enhanced chemical sinks

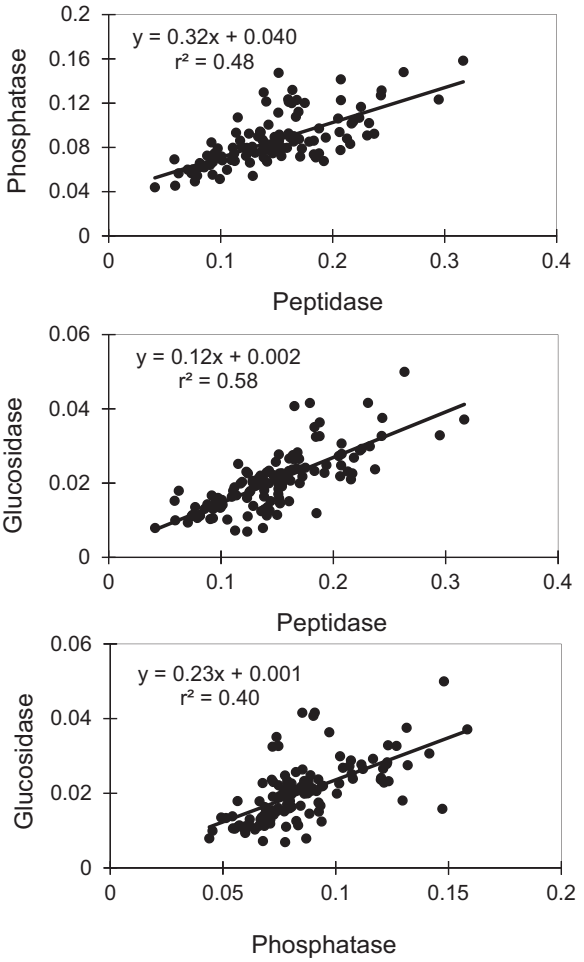

Figure 11. Comparison of the activities of the three classes of enzymes with each other during all sampling seasons and associated coefficients of determination.

for phosphate. A weak but significant correlation (<0.01) was found between LAP/PA versus N/P indicating a decreased phosphate supply and potential phosphate deficiency.

As noted previously, a major reason that EEA correlates with metabolite production rate but not product solute concentrations is the different transport processes affecting particles and solutes. EEA measures the instantaneous rate of substrate hydrolysis associated with reactive particle distributions. Reactive particle transport occurs on slower time scales than solute transport and by different mechanisms, for example, particle reworking and sedimentation. Solute concentrations are strongly affected by diffusion and bioirrigation in addition to production and consumption reactions. The sediment-water interface region demonstrates

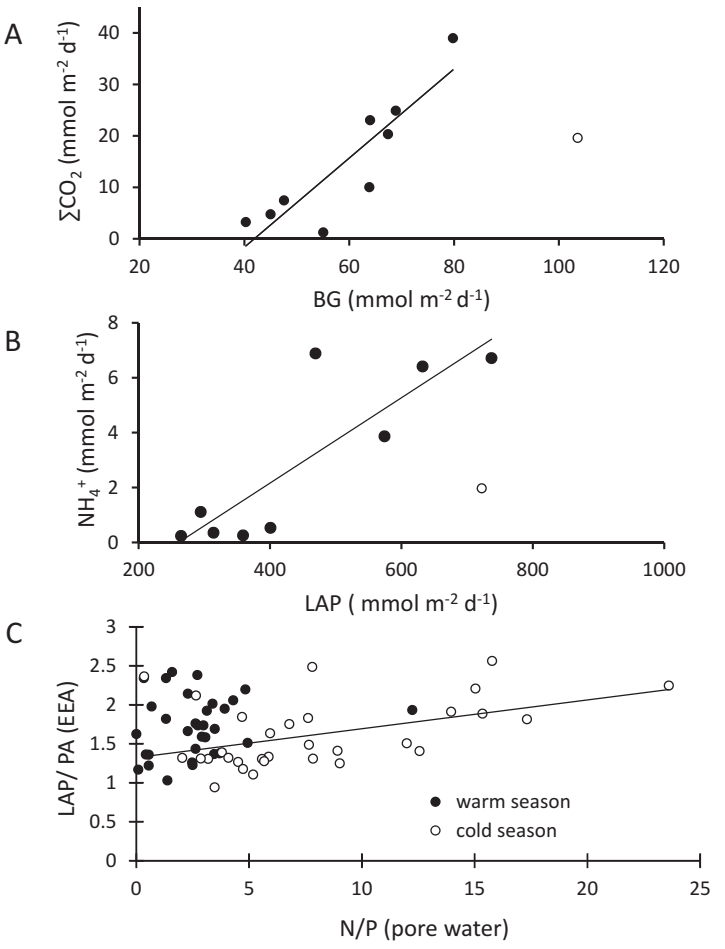

Figure 12. Extracellular enzyme activities versus their respective end member nutrient production rates: Type 2 (geometric mean) regressions for (a) β-glucosidase (BG) and ΣCO_2 production (integrated as equivalent flux $\Sigma CO_2 = 0.87\,(BG) - 36.2$; $r^2 = 0.79$), (b) leucine aminopeptidase (LAP) and NH_4 production (NH_4^+ flux $= 0.0068(LAP) - 1.76$; $r^2 = 0.73$), and (c) nitrogen-phosphorous ratio (N/P) and leucine aminopeptidase -phosphatase ratio (LAP/PA) where there is no clear relationship although N/P is lower during the warmer seasons compared with that in colder seasons.

these differences directly: the most reactive substrate is present and decomposition rates are often highest, but metabolite levels (for example, ΣCO_2) are usually minimal due to diffusive losses into contacting overlying water.

Another interesting relationship between metabolite production rates and EEA is that the regression intercepts suggest measureable EEA in the absence of net metabolite production

into pore water (Figs. 12a, b). These intercepts may reflect the level of EEA required to support biomass synthesis (e.g., incorporation of NH_4^+ into biomass rather than release to solution), or may be artifacts of the measurement methods since the current techniques measure EEA maximum potential.

5. Conclusions

Sedimentary extracellular enzyme activity (EEA) varies seasonally in estuarine sediments of Great Peconic Bay: highest during the spring bloom and summer, and lowest during the fall and early winter. Seasonal variation is determined by both temperature and the availability of reactive organic substrates, with EEA varying directly with both. Although traditional EEA measurements document these overall seasonal patterns, high resolution, 2-D EEA distributions, obtained using a novel optical sensor that preserves sedimentary structure, reveal controlling factors, substrate transport patterns, and metabolic phenomena more accurately and in ways not possible using traditional slurry techniques. A high degree of horizontal heterogeneity in EEA was present, particularly during warm seasons. Hot spots of metabolic activity associated with aggregates of reactive organic material can be discriminated statistically. These microniches of enhanced EEA were most obvious during initial penetration of reactive detritus into underlying sediment following the spring bloom, and around burrow structures during other times. EEA is closely associated with metabolites (pCO_2) when bioturbation is minimal, for example, in the highly reactive fluff layer deposited as a pulse during the spring bloom. However, EEA and solute build up patterns are decoupled during much of the year because of the different transport mechanisms and rates of transport affecting reactive particle substrates and solutes in bioturbated deposits. EEA correlates directly with depth-integrated remineralization rates (ΣCO_2, NH_4^+ production). The 2-D EEA methodology provides a unique means to directly and independently measure the complex, unsteady processes affecting reactive organic matter substrate distributions in both oxic and anoxic zones of sedimentary deposits.

Acknowledgments. We thank C. Wall for assistance in collection of core samples and C. Heilbrun and S. Rahman for assistance in the laboratory. We also thank the editor and two anonymous reviewers for their constructive comments, which helped us improve the manuscript. Funding for this study came from NSF grants OCE 0851207 and OCE 1332418, and NY State Sea Grant R/CMC-8.

REFERENCES

Aller, J. Y. and R. C. Aller 1986. Evidence for localized enhancement of biological activity associated with tube and burrow structures in deep-sea sediments at the HEBBLE site, Western North Atlantic. Deep-Sea Res., *33*, 6, 755–790.

Aller, R. C. 1994. Bioturbation and remineralization of sedimentary organic-matter-effects of redox oscillation. Chem. Geol., *114*, 3–4, 331–345.

Aller, R. C. (2001) Transport and reactions in the bioirrigated zone, in The Benthic Boundary Layer: Transport Processes and Biogeochemistry, edited by B. P. Boudreau and B. B. Jorgensen, B.B, pp. 269–301, Oxford Press.

Aller, R. C. and J. Y. Aller. 1998. The effect of biogenic irrigation intensity and solute exchange on diagenetic reaction rates in marine sediments. J. Mar. Res., *56*, 4, 905–936.

Aller, R. C. and J. E. Mackin. 1989. Open-incubation, diffusion methods for measuring solute reaction-rates in sediments. J. Mar. Res., *47*, 2 411–440.

Arnosti, C. 1995. Measurement of depth-related and site-related differences in polysaccharide hydrolysis rates in marine-sediments. Geochim. Cosmochim. Ac., *59*, 20, 4247–4257.

Arnosti, C. 2011. Microbial extracellular enzymes and the marine carbon cycle, in Annual Review of Marine Science, Vol 3, edited by C. A. Carlson and S. J. Giovannoni, pp. 401–425, Annual Review of Marine Science.

Arnosti, C., D. J. Repeta and N. V. Blough. 1994. Rapid bacterial degradation of polysaccharides in anoxic marine systems. Geochim. Cosmochim. Ac., *58*, 12, 2639–2652.

Baltar, F., J. Arístegui, E. Sintes, H. M. Van Aken, J. M. Gasol and G. J. Herndl. 2009. Prokaryotic extracellular enzymatic activity in relation to biomass production and respiration in the meso- and bathypelagic waters of the (sub)tropical Atlantic. Environ. Microbiol., *11*, 8, 1998–2014.

Belanger, C., B. Desrosiers and K. Lee. 1997. Microbial extracellular enzyme activity in marine sediments: extreme pH to terminate reaction and sample storage. Aquat. Microb. Ecol., *13*, 2, 187–196.

Bertics, V. J. and W. Ziebis. 2009. Biodiversity of benthic microbial communities in bioturbated coastal sediments is controlled by geochemical microniches. The ISME Journal, *3*, 1269–1285.

Boetius, A., 1995. Microbial hydrolytic enzyme activites in deep-sea sediments. Helgol. Meeresunters., *49*, 1–4, 177–187.

Boetius, A. and K. Lochte. 1994. Regulation of microbial enzymatic degradation of organic matter in deep-sea sediments. Mar. Ecol.-Prog. Ser., *104*, 3, 299–307.

Breuer, E., S. A. Sanudo-Wilhelmy and R. C. Aller. 1999. Trace metals and dissolved organic carbon in an estuary with restricted river flow and a brown tide bloom. Estuaries, *22*, 3A, 603–615.

Bruno, S. F., R. D. Staker and G. M. Sharma. 1980. Dynamics of phytoplankton productivity in the Peconic Bay Estuary, Long Island. Estuar. Coast. Mar. Sci., *10*, 3, 247–263.

Burdige, D. J. and K. G. Gardner. 1998. Molecular weight distribution of dissolved organic carbon in marine sediment pore waters. Mar. Chem., *62*, 1–2, 45–64.

Cao, Z. R., Q. Z. Zhu, R. C. Aller, and J. Y. Aller. 2011. A fluorosensor for two-dimensional measurements of extracellular enzyme activity in marine sediments. Mar. Chem., *123*, 1–4, 23–31.

Chrost, R. J. 1991. Environmental control of the synthesis and activity of aquatic microbial ectoenzymes, in: Microbial Enzymes in Aquatic Environments, edited by R. J. Chrost, Springer-Verlag, New York.

Doane, T. A., and W. R. Horwath. 2003. Spectrophotometric determination of nitrate with a single reagent. Anal. Lett., *36*, 12, 2713–2722.

Gerino, M., R. C. Aller, C. Lee, J. K. Cochran, J. Y. Aller, M. A. Green and D. Hirschberg. 1998. Comparison of different tracers and methods used to quantify bioturbation during a spring bloom: 234-thorium, luminophores and chlorophyll a. Estuar. Coast. Shelf Sci., *46*, 4, 531–547.

Glud, R. N. 2008. Oxygen dynamics of marine sediments. Mar. Biol. Res., *4*, 4, 243–289.

Glud, R. N., N. B. Ramsing, J. K. Gundersen, and I. Klimant. 1996. Planar optrodes: a new tool for fine scale measurements of two-dimensional O_2 distribution in benthic communities. Mar. Ecol. Prog. Ser., *140*, 1–3, 217–226.

Glud, R. N., F. Wenzhöfer, A. Tengberg, M. Middelboe, K. Oguri and H. Kitazato, H. 2009. In situ microscale variation in distribution and consumption of O_2: a case study from a deep ocean margin sediment (Sagami Bay, Japan). Limnol. Oceanogr., *54*, 1, 1–12.

Glud, R. N., A. Tengberg, M. Kühl, P. O. Hall, I. Klimant and G. Hoist. 2001. An in situ instrument for planar O_2 optode measurements at benthic interfaces. Limnol. Oceanogr., *46*, 8, 2073–2080.

Graf, G. 1992. Benthic-pelagic coupling—a benthic view. Oceanogr. Mar. Biol., *30*, 149–190.

Hall, P. O., and R. C. Aller. 1992. Rapid, small-volume, flow-injection analysis for S-CO_2 and NH_4^+ in marine and fresh-waters. Limnol. Oceanogr., *37*, 5, 1113–1119.

Hansen, J. W., B. Thamdrup and B. B. Jorgensen. 2000. Anoxic incubation of sediment in gas-tight plastic bags: a method for biogeochemical process studies. Mar. Ecol.-Prog. Ser., *208*, 273–282.

Hill, B. H., C. M. Elonen, T. M. Jicha, D. W. Bolgrien, and M. F. Moffett. 2010. Sediment microbial enzyme activity as an indicator of nutrient limitation in the great rivers of the Upper Mississippi River basin. Biogeochem., *97*, 2–3, 195–209.

Hobbie, J. E., R. J. Daley and S. Jasper. 1977. Use of nuclepore filters for counting bacteria by fluorescence microscopy. Appl. Environ. Microb., *33*, 5, 1225–1228.

Hoppe, H. G. 1983. Significance of exoenxymatic activities in the ecology of brackish water measurments by means of methylumbelliferyl substrates. Mar. Ecol.-Prog. Ser., *11*, 3, 299–308.

Hoppe, H. G. 2003. Phosphatase activity in the sea. Hydrobiologia, *493*, 1–3, 187–200.

Hoppe, H. G., C. Arnosti and G. J. Herndl. 2002. Ecological significance of bacterial enzymes in the marine environment, in Enzymes in the Environment, edited by R. G. Burns and R. P. Dick, pp. 73–107, Marcel Dekker, New York.

Hoppe, H. G. and S. Ullrich. 1999. Profiles of ectoenzymes in the Indian Ocean: phenomena of phosphatase activity in the mesopelagic zone. Aquat. Microb. Ecol., *19*, 2, 139–148.

Hulthe, G., S. Hulth and P. O. J. Hall. 1998. Effect of oxygen on degradation rate of refractory and labile organic matter in continental margin sediments. Geochim. Cosmochim. Acta, *62*, 8, 1319–1328.

Hunt, C. D. 1983. Variability in the benthic Mn flux in coastal marine ecosystems resulting from temperature and primary production. Limnol. Oceanogr., *28*, 5, 913–923.

Huston, A. L. and J. W. Deming. 2002. Relationships between microbial extracellular enzymatic activity and suspended and sinking particulate organic matter: seasonal transformations in the North Water. Deep-Sea Res., *49*, 22–23, 5211–5225.

Jorgensen, B. B. 1977. Bacterial sulfate reduction within reduced microniches of oxidized marine-sediments. Mar. Biol., *41*, 1, 7–17.

Katuna, M. P. 1974. The Sedimentology of Great Peconic Bay and Flanders Bay, LI, NY. PhD dissertation, Queens College, Department of Earth and Environmental Sciences.

Kristensen, E., and J. E. Kostka. 2005. Macrofaunal burrows and irrigation in marine sediment: microbiological and biogeochemical interactions, in Interactions between Macro- and Microorganisms in Marine Sediments, edited by E. Kristensen, R. R. Haese and J. E. Kostka, pp. 125–157, Coastal and Estuarine Studies, American Geophysical Union.

Lonsdale, D. J., D. I. Greenfield, E. M. Hillebrand, R. Nuzzi and G. T. Taylor. 2006. Contrasting microplanktonic composition and food web structure in two coastal embayments (Long Island, NY, USA). J. Plankton Res., *28*, 10, 891–905.

Mackin, J. E. and R. C. Aller. 1984. Ammonium Adsorption in Marine-Sediments. Limnol. Oceanogr., *29*, 2, 250–257.

Mayer, L. M. 1989. Extracellular proteolytic-enzyme activity in sediments of an intertidal mudflat. Limnol. Oceanogr., *34*, 6, 973–981.

Meyerreil, L. A. 1986. Measurement of hydrolytic activity and incorporation of dissolved organic subtrates by microorganisms in marine sediments. Mar. Ecol.-Progr. Ser., *31*, 2, 143–149.

Miranda, K. M., M. G. Espey and D. A. Wink. 2001. A rapid, simple spectrophotometric method for simultaneous detection of nitrate and nitrite. Nitric Oxide-Biol. Ch., *5*, 1, 62–71.

Papaspyrou, S., T. Gregersen, E. Kristensen, B. Christensen and R. P. Cox. 2006. Microbial reaction rates and bacterial communities in sediment surrounding burrows of two nereidid polychaetes (Nereis diversicolor and N-virens). Mar. Biol., *148*, 3, 541–550.

Poremba, K. and H. G. Hoppe. 1995. Spatial variation of benthic microbial production and hydrolytic enzymatic activity down the continental slope of the Celtic Sea. Mar. Ecol.-Prog. Ser., *118*, 1–3, 237–245.

Presley, B. J. 1971. Determination of selected minor and major inorganic constituents. Initial Rep. Deep Sea, *7*, 5, 1749–1755.

Solorzano, L. 1969. Determination of ammonia in natural waters by phenolhypochlorite method. Limnol. Oceanogr., *14*, 5, 799–01.

Volkenborn, N., C. Meile, L. Polerecky, C. A. Pilditch, A. Norkko, J. Norkko, J. E. Hewitt, et al. 2012. Intermittent bioirrigation and oxygen dynamics in permeable sediments: an experimental and modeling study of three tellinid bivalves. J. Mar. Res., *70*, 794–823.

Watson, S. W., T. J. Novitsky, H. L. Quinby and F. W. Valois. 1977. Determination of bacterial number and biomass in marine enviornment. Appl. Environ. Microb., *33*, 4, 940–946.

Weiss, M. S., U. Abele, J. Weckesser, W. U. Welte, E. Schiltz and G. E. Schulz. 1991. Molecular architecture and electrostatic properties of a bacterial porin. Science, *254*, 5038, 1627–1630.

Wenzhofer, F. and R. N. Glud. 2004. Small-scale spatial and temporal variability in coastal benthic O_2 dynamics: effects of fauna activity. Limnol. Oceanogr., *49*, 5, 1471–1481.

Zhu, Q. Z. and R. C. Aller. 2010. A rapid response, planar fluorosensor for measuring two-dimensional pCO_2 distributions and dynamics in marine sediments. Limnol. Oceanogr.-Methods, *8*, 326–336.

Zhu, Q. Z., R. C. Aller and Y. Z. Fan. 2005. High-performance planar pH fluorosensor for two-dimensional pH measurements in marine sediment and water. Environ. Sci. Technolo., *39*, 22, 8906–8911.

Zhu, Q. Z., R. C. Aller and Y. Z. Fan. 2006. Two-dimensional pH distributions and dynamics in bioturbated marine sediments. Geochim. Cosmochim. Acta, *70*, 19, 4933–4949.

Received: *16 January 2013*; revised: *21 February 2014*.